PROCEEDINGS OF THE INTERNATIONAL CONFERENCE
NANOMATERIALS: APPLICATIONS AND PROPERTIES
Vol. 2 No 1, 01NTF07(5pp) (2013)

Investigation on the Structural and Optical Properties of Thermally Evaporated Indium Selenide Compound Material for Solar Cell Application

A. Mohan, J. Suthagar, T. Mahalingam

Thin Film Laboratory, Department of Physics, Karunya University, Coimbatore-641114, India

(Received 17 May; published online 30 August 2013)

In_2Se_3 thin films with different thicknesses have been deposited by thermal evaporation method on glass substrate under vacuum pressure of 10^{-6} Torr. Structural Properties of these films were studied by different analytical techniques. X- ray diffraction revealed as deposited films have amorphous nature and annealing effect enhanced crystalline structure. Structural studies by XRD results showed the polycrystalline nature of the films. The Full Width at Half Maximum (FWHM) values were observed from the XRD pattern and used to evaluate the microstructural parameters like crystallite size, strain, dislocation density. The optical absorption spectra of In_2Se_3 films were studied in the wavelength region of 250–2500 nm. The optical properties show that the band gap (Eg) values vary from 2.5 to 3.34 eV as annealing temperature varies from 150 to 350°C.

Keywords: In_2Se_3, Thermal Evaporation, XRD, Amorphous, Polycrystalline.

PACS number(s): 81.15.Ef, 68.55 –a, 78.20 -e

1. INTRODUCTION:

Indium Selenide (In_2Se_3) is one of the promising materials of chalcogenide alloys from the III – VI group semiconductor. Because of the better heterojunction with the In_2Se_3/CIS layer than the CdS/CIS layer combination [1], In_2Se_3 thin films are used in Diode [2], photo electrochemical application [3], Phase change random access memory (PRAM) [4] and used as a buffer layer for CIS solar cells. Also indium selenide is used as window layer (γ-In_2Se_3) and absorber layer (β-In_2Se_3) in solar cells depending on optical band gap of thin films. γ-In_2Se_3 (window layer) with wide band gap 1.8 eV is greater than β-In_2Se_3 (absorber layer) and InSe having a band gap 1.55 eV [5]. So far many techniques are used to prepare Indium Selenide thin films such as chemical bath deposition [6], Mechanical Alloying Techniques [7], MOCVD [8], Spray pyrolysis [9], sol gel method [10] and LP – LAPW method [11]. Among these methods, thermal evaporation is a promising method to prepare high quality semiconductor thin films. Many researchers investigated by this technique, but most of them concentrating on bilayer of In and Se stack deposition.

In this present work we have prepared thin films of thermally evaporated Indium Selenide compound material and then studied structural and optical properties of Indium Selenide thin films with various thicknesses and at different annealing temperatures.

2. EXPERIMENTAL PROCEDURE

In_2Se_3 thin films were prepared by evaporating In_3Se compound. Indium Selenide compound was kept in Molybdenum boat and then deposited on ultrasonically cleaned unheated soda lime glass substrates under the vacuum pressure of 10^{-6} torr. The successive film coatings of different thicknesses are 100 nm, 200 nm and 300 nm and film thickness was maintained by using thickness monitor. A constant rate of evaporation ranging 1-3 Å/sec was maintained throughout the deposition process. Then films were annealed under open air atmosphere at 150°C, 250°C and 350°C for about 30 minutes. The X-ray diffraction studies of both as deposited and annealed In_2Se_3 films were carried out using Shimadzu XRD-6000 X-ray Diffractometer. Here the films were exposed to Cu Kα source and the scattering angles were varied from 0 - 90°. The optical studies of the prepared films were analysed using UV-VIS-NIR spectrophotometer (Jasco-570 UV/VIS/NIR Spectrophotometer) in the range of 200 to 2500 nm.

3. RESULTS AND DISCUSSIONS

3.1 X-ray diffraction

The X-ray diffraction (XRD 6000) studies are carried out for these samples, to find effects of thickness and annealing temperature on structure of InSe thin films.

Fig 1 shows that recorded XRD pattern of as deposited, and annealed films of thickness 100 nm , which revealed that as deposited and annealed at 150°C, 250°C films exhibits amorphous nature. Further annealing at 350°C films enhanced crystalline nature. The prominent peaks corresponding to (4 1 0) plane was observed in the film. This recorded XRD pattern were compared with the JCPDS data (card number: 83-0039) which confirm the orthorhombic crystal structure of In_4Se_3.

The XRD pattern of annealed at 350°C films with thicknesses of 200 nm and 300 nm, shown in Fig 2 and 3, have well grown orientation along (1 1 0), (3 0 0) and (2 0 2). These were compared with JCPDS data (card number: 89-0658), which confirmed hexagonal structure and presence of γ-In_2Se_3 and also similar peaks are found previous result. From XRD pattern 3 (250°C) films show peak at (3 0 0) orientation, this confirms formation of γ-In_2Se_3. Annealing effect enhanced crystalline quality and increases the grain size.

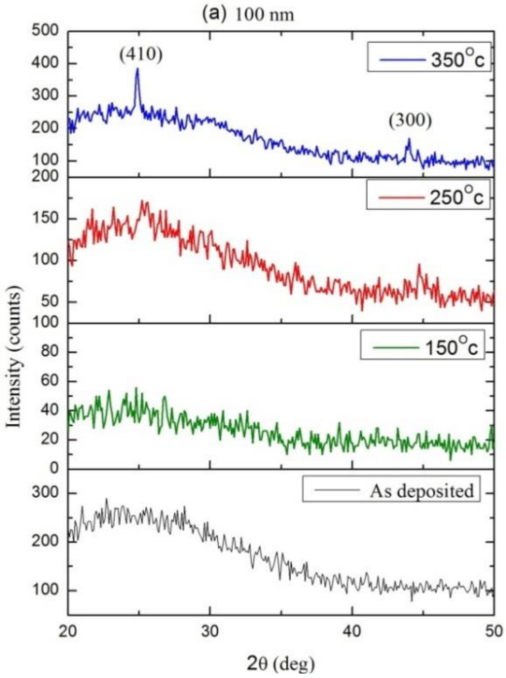

Fig. 1 – XRD pattern of InSe film of thickness 100 nm at different annealed temperatures

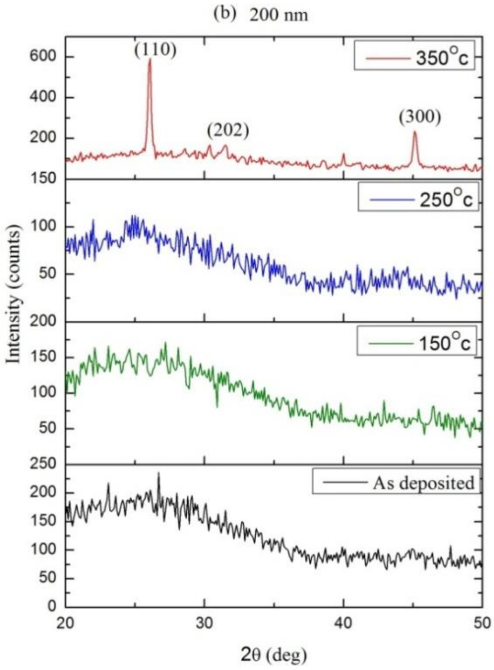

Fig. 2 – XRD pattern of InSe film of thickness 200 nm at different annealed temperatures

The crystalline size (D) was calculated using Scherer's formula [12]

$$D = \frac{0.94\lambda}{\beta \cos\theta} \tag{1}$$

where λ is the wavelength of the X-ray beam used, 2θ is the angle between the incident and scattered X-ray beam and β is the full width at half maximum (FWHM) and the dislocation density is estimated from the relation

$$\delta = \frac{1}{D^2} \tag{2}$$

The number of crystallites per unit area (N) of the film was determined by using formula [13]

$$N = \frac{t}{D^3} \tag{3}$$

where t is thickness of the film.

The micro strain (ε) developed in the InSe film is calculated from the relation

$$\varepsilon = \beta \cos\Theta / 4 \tag{4}$$

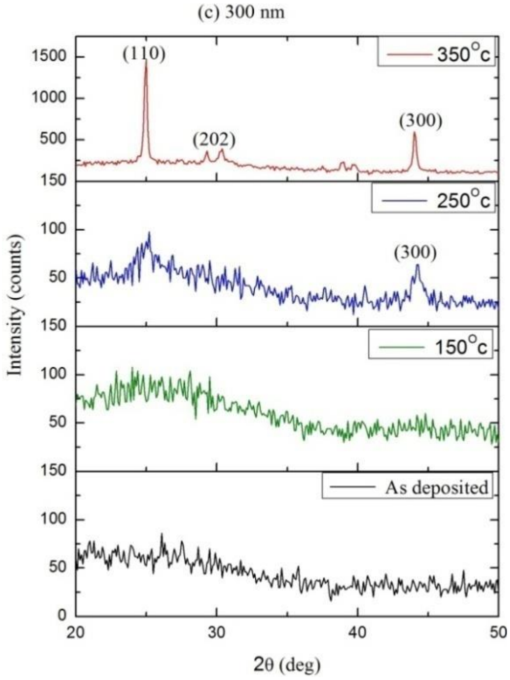

Fig. 3 – XRD pattern of InSe film of thickness 300nm at different annealed temperatures

Structural parameter of Indium Selenide films annealed at 350°C shown in table 1. Increasing average grain size shows peaks are growing very narrow and decrease dislocation density, micro strain has improving crystalline structure. From above result increase grain size and decrease dislocation density, micro strain, number of crystallites show annealing at 350°C films have good crystalline structure than other films.

Broader full width half maximum has very small grain and smaller FWHM have larger grain size. From the above XRD pattern we confirmed that a larger grain has very small FWHM and also thickness is an important parameter to prepare good crystalline films.

3.2 Optical Studies

Optical absorption and transmission of Indium Selenide films deposited onto soda lime glass was recorded using UV-VIS-NIR spectrophotometer (Jasco-570 UV/VIS/NIR Spectrophotometer) in the range of 200 to 2500 nm. The transmission spectra of the films as deposited and annealed at different temperature (150 °C - 350 °C) with various thickness is shown in fig. 4.

Table 1 – Structural parameters of InSe thin films annealed at 350°C

Thickness, nm	2θ	d	FWHM	Average Grain size, D nm	Dislocation density (10^{18} nm^{-2})	N, 10^{18}/m^2	Strain ε
100	24.30 22.02 29.60	3.6598 4.0189 3.0155	4.0000 4.5000 3.6500	2.1	0.226	10.7	0.0976
200	24.927 44.001 30.315	3.5691 2.0562 2.9460	0.3096 0.3265 0.4051	4.4	0.053	2.34	0.083
300	24.937 44.011 29.278	3.5677 2.0557 3.0478	0.3043 0.3093 0.3242	4.8	0.043	2.71	0.075

As deposited films higher transmission than annealing films and also interference pattern was formed by increasing thickness shown in Fig 4. Film thickness and annealing temperature played important role in the transmission spectrum by reducing transmission. The extinction coefficient can be calculated from the formula [14]:

$$k = \frac{\ln\left(\frac{1}{T}\right)\lambda}{4\pi t} \qquad (5)$$

where t is the thickness of the deposited film.

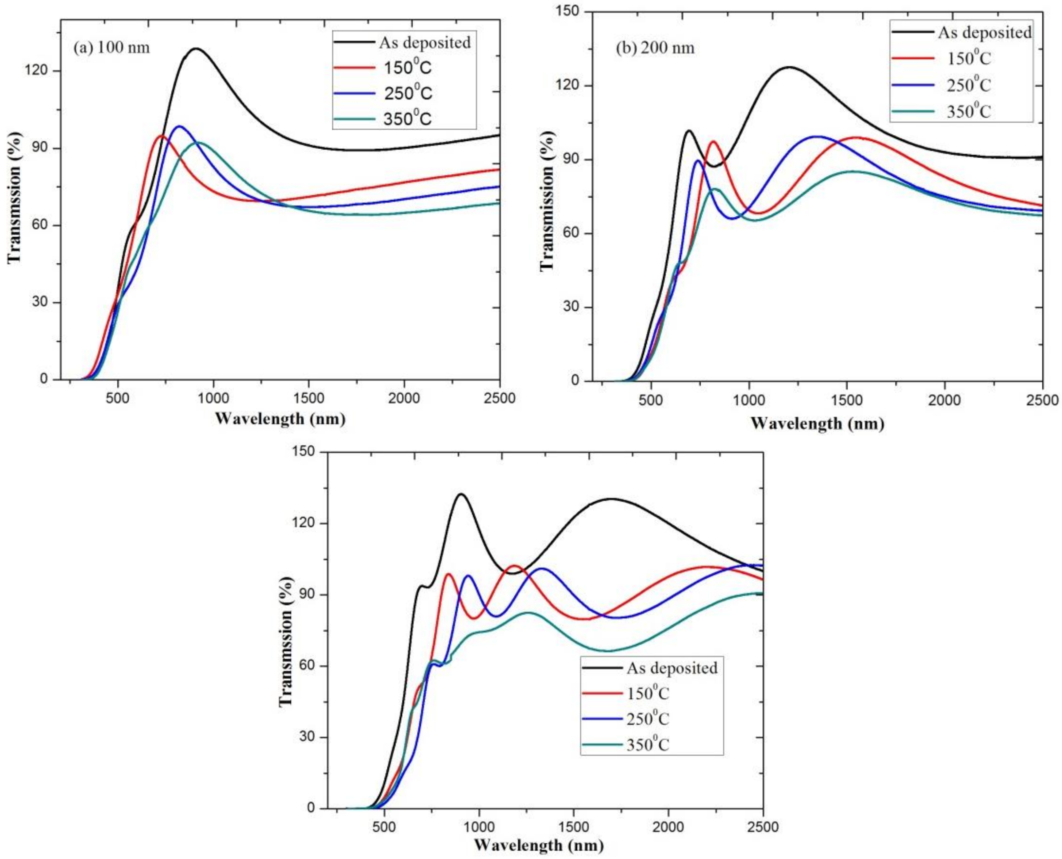

Fig 4. – Transmission spectra of InSe thin films (a) 100 nm, (b) 200nm and (300nm)

Energy band gap of InSe thin films were calculated by using optical transmission spectra. To find energy band gap, we plotted graph (hυ) vs. $(\alpha h\upsilon)^2$ where α is absorption coefficient of the film and hυ is photon energy. The nature of the transition can be investigated on the basis of the dependence of the absorption coefficient with the incident photon energy hυ.

$$(\alpha h)^2 = A(h\upsilon - E_g)^n \qquad (6)$$

where hυ is the incident photon energy, A is a constant and the exponent n depends on the type of transition, n = 0.5 for direct transition. The optical band gap of these films was determined by extrapolating the linear portion of the curve to the energy axis at $(\alpha h\upsilon)^2 = 0$. Hence, the direct optical band gap E_g can be evaluated from the plot of $(\alpha h\upsilon)^2$ vs hυ.

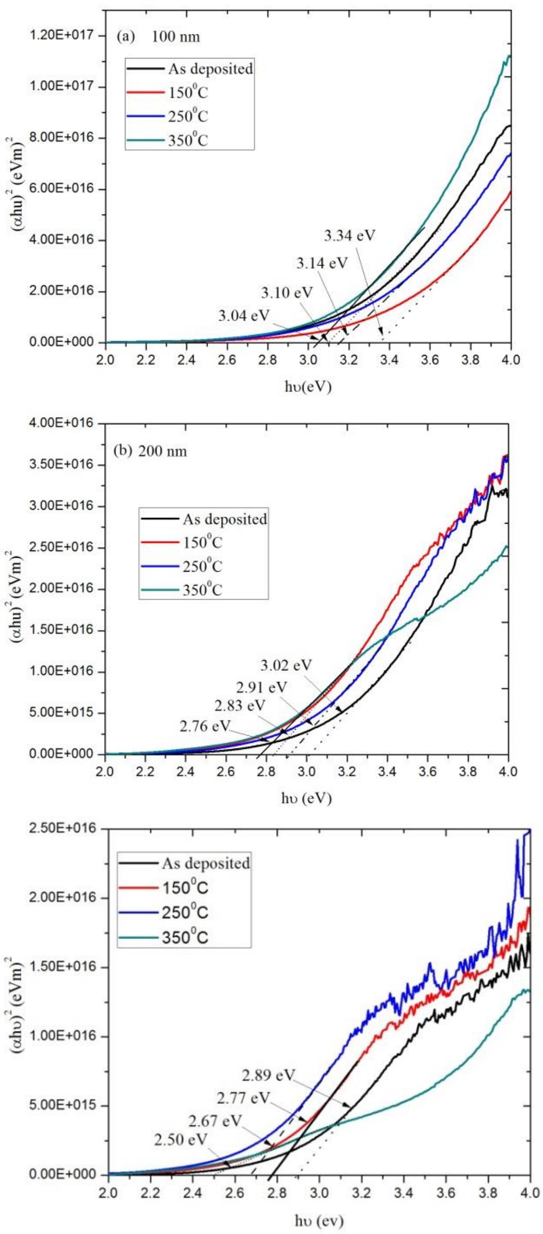

Fig. 5 – Energy Band Gap of InSe (a) 100 nm, (b) 200nm and (300nm) (c)

The absorption coefficient can be calculated from the following the relation:

$$\alpha = \frac{4\pi k}{\lambda} \quad (7)$$

The absorption coefficient of different thickness of InSe thin films plotted against wavelength and the graph is shown in Fig.6.

Fig.6 clearly shows that the absorption coefficient was maximum for high In content and minimum for the low In content [17]. Lower thickness InSe films have more indium content than higher thickness films, which is confirmed from XRD pattern.

The direct band gap of the films deposited at different thicknesses was found to be in the range from 3.34 to 2.50eV. The values of the estimated energy gap for amorphous films are greater than that obtained for crystalline InSe films, because in the polycrystalline material the electron transition is from band to band. But in amorphous materials the electron transitions may be either from localized states at the valance band edge to extended states in the conduction band or from extended states in the valance band to the localized states at the conduction edge. This leads to higher energies than those for polycrystalline materials. The energy band gap value was found to decrease with an increase in film thickness and annealing temperature. Decrease in energy band may be formation of γ - In_2Se_3 phase, which has larger band gap than previous results [15]. Formation of γ - In_2Se_3 phase confirmed from the XRD pattern.

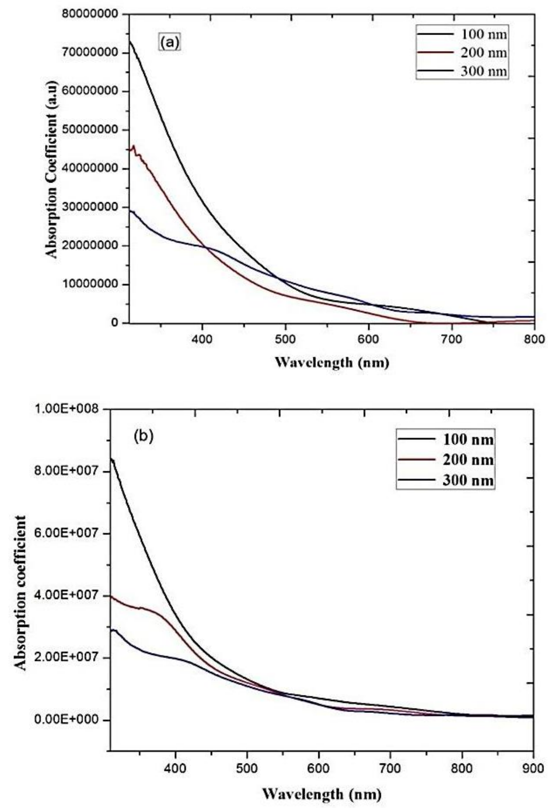

Fig. 6 – Absorption coefficient of InSe films (a) as deposited and (b) annealing at 350°C

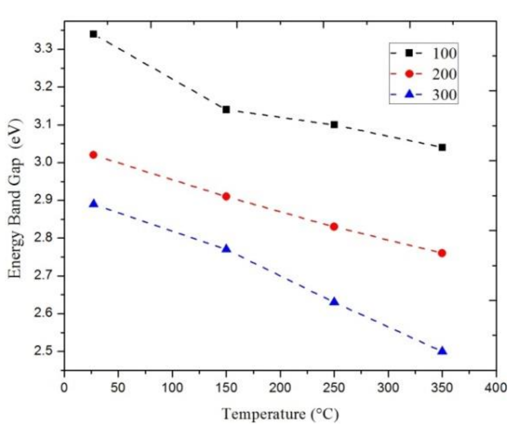

Fig. 7 – Energy band gap of InSe films with annealing temperature

The variation of energy band gap of InSe thin films with annealing temperature is shown in Fig 7. Films annealed at higher temperature are established lower band gap. This may be due to Sharpe edges in crystalline films. The decrease of band gap with increase of annealing temperature is attributed to increase of grain size and decrease in micro strain [16].

Fig. 8 shows the optical band gap value decreases with an increase in film thickness due to an increase of particle size and decrease in micro strain. This is further explained from the three dimensional quantum size effects leading to decrease band gap with increase in particle size, which is well known for colloidal semiconductor.

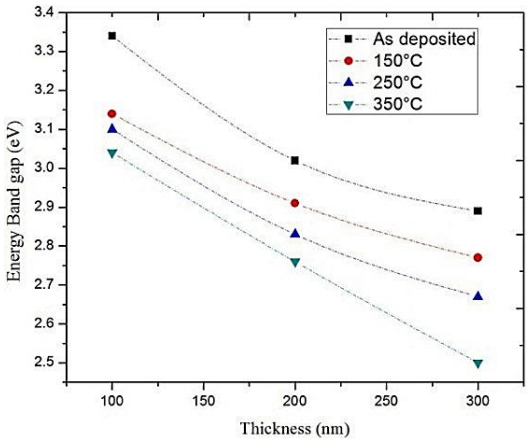

Fig. 8 – Energy band gap of InSe films with different thicknesses

4. CONCLUSION

Indium Selenide thin films have been prepared by thermal evaporation techniques on ultrasonically cleaned glass substrate. The annealing effect on structural and optical band gap has been studied. As deposited and annealed at lower temperature shows amorphous nature and annealed at 350°C films have hexagonal structure. This confirms that annealing effect enhances crystalline quality. It is observed that optical band gap decrease 3.34eV to 2.50eV and which arise grain growth upon annealing. This is because of the formation of γ- In_2Se_3 phase, which has wider band gap for annealed films.

ACKNOWLEDGMENT

The authors are grateful to the Central Research Facility, Karunya University for supporting of this work.

REFERENCES

1. G. Gordillo, C. Calderon, *Solar Energy Material and Solar Cells*,**77,** 163 (2003).
2. Atsufumi Hirohata, Jagadeesh S. Moodera, Geetha P. Berera, *Thin Solid Films* **510**, 247 (2006).
3. K. C. Rathod , M. R. Asabe ,A. V. Jadhav , V. B. Helavi , S. S. Chavan ,K. M. Garadkar , I. S. Mulla , P. P. Hankare, *J. Mater Sci: Mater Electron,* **22**, 359 (2011).
4. Heon Lee, Dae Hawan Kang, Lung Tran, *Mater. Sci. and Eng. B,* **119** 196 (2005).
5. R. Sreekumar, R. Jayakrishnan, C. Sudha kartha, K. P. Vijjyakumar, Y. Kashibawa and T. Abe, , *Solar Energy Material and Solar Cell,* **90,** 298 (2006).
6. K. Bindu, C. Sudha Kartha, K.P. Vijayakumar, T. Abe, Y. Kasiwaba, *App. Surf. Sci.* **191**, 138 (2002).
7. S.M. El-Sayed, *Vacuum* **72**, 169 (2004).
8. Mohammad Afzaal, David Crouch, Paul O'Brien, *Mater. Sci. and Eng.* B **116,** 391 (2005).
9. Teny Theresa Johna, C. Sudha Karthaa, K.P. Vijayakumara, T. Abeb, Y. Kashiwaba, *Vacuum* **80,** 870 ((2006)).
10. Ibrahim H. Mutlu , Maharram Z. Zarbaliyev , Ferhat Aslan, *J. of Sol-Gel Sci. and Tech.,* **43**, 233 (2007).
11. T. BenNasr n, H.BenAbdallah, R.Bennaceur, *Physica B* **405**, 3427 (2010).
12. S. Venkatachalam, Y.L. Jeyachandrn, P. Suresh Kumar, A. Dhayalraj, D. Mangalaraj , Sa.K. Narayandass, S. Velumani, *Mater. Charact.* **58,** 794 (2007).
13. T. Mahalingam, V. Dhanasekaran, R. Chandramohan, Jin-Koo Rhee, *J. of Mater. Sci.,* **47**, 1950 (2012).
14. Viswanathan, S. Gopal, D. Mangala Raj, Sa. K. Naryanadass, O.F. Caltun, G. Rusu and Junsin Yi, *Ionic,* **10** (2004).
15. Aytunc Ates, Muthu Kundac1, Aykut Astam, *Physica E* **40**, 2709 (2008).
16. S.Agilan, D. Mangalaraj, Sa. K. Narayandass, G. Mohan Rao, *Physica B,* 93 (2005).